Appl. Phys. A (2016) 122:1058
DOI 10.1007/s00339-016-0577-7

Applied Physics A
Materials Science & Processing

Shellac/nanoparticles dispersions as protective materials for wood

Maduka L. Weththimuni[1] · Doretta Capsoni[1] · Marco Malagodi[2,3] · Chiara Milanese[1] · Maurizio Licchelli[1,2]

Received: 23 June 2016 / Accepted: 17 November 2016 / Published online: 29 November 2016

Abstract Wood is a natural material that finds numerous and widespread applications, but is subject to different decay processes. Surface coating is the most common method used to protect wood against deterioration and to improve and stabilize its distinctive appearance. Shellac is a natural resin that has been widely used as a protective material for wooden artefacts (e.g. furniture, musical instruments), due to its excellent properties. Nevertheless, diffusion of shellac-based varnishes has significantly declined during the last decades, because of some limitations such as the softness of the coating, photo-degradation, and sensitivity to alcoholic solvents and to pH variations. In the present study, different inorganic nanoparticles were dispersed into dewaxed natural shellac and the resulting materials were investigated even after application on wood specimens in order to assess variations of the coating properties. Analyses performed by a variety of experimental techniques have shown that dispersed nanoparticles do not significantly affect some distinctive and desirable features of the shellac varnish such as chromatic aspect, film-forming ability, water repellence, and adhesion. On the other hand, the obtained results suggested that some weak points of the coating, such as low hardness and poor resistance to UV-induced ageing, can be improved by adding ZrO_2 and ZnO nanoparticles, respectively.

✉ Maurizio Licchelli
maurizio.licchelli@unipv.it

[1] Department of Chemistry, University of Pavia, via Taramelli 12, 27100 Pavia, Italy

[2] CISRiC-Arvedi Laboratory of Non-Invasive Diagnostics, University of Pavia, via Bell'Aspa 3, 26100 Cremona, Italy

[3] Department of Musicology and Cultural Heritage, University of Pavia, Corso Garibaldi 178, 26100 Cremona, Italy

1 Introduction

Wood is an organic material that undergoes different degradation processes due to environmental agents (e.g. solar radiation, water, temperature variations). Protection of wood from external decay factors can be pursued by different methods, such as surface coatings, chemical modification, and impregnation with chemicals [1, 2]. Nevertheless, surface covering with different kinds of coatings still represents the most common practice for wood protection. For instance, wooden furniture and musical instruments are usually coated with a protective layer that plays also an aesthetic role, and in the case of stringed instruments, it is supposed to affect the acoustical features as well [3].

At present, most coatings for wood are based on synthetic polymers (e.g. polyurethanes, polyesters, polyacrylates), which show excellent properties from many points of view. However, many polymeric materials display also some weak points such as unsatisfactory resistance to wearing [4] and high environmental impact.

Shellac is a natural thermosetting resin of animal origin secreted by Lac insects (e.g. Kerria Lacca, Laccifer Lacca), mostly growing over host trees in China, India, Myanmar, and Thailand [5–8]. Shellac consists of an intimate mixture of several polar and non-polar components: Resinous material is always associated with an odoriferous compound, a waxy component, and a mixture of dyes such as erythrolaccin and desoxyerythrolaccin, which are hydroxyanthraquinone derivatives [9]. The resin portion of shellac is made by a complex mixture of esters (about 30%, soft resin) and polyesters (about 70%, hard resin) deriving from sesquiterpenic and hydroxy fatty acids [7, 9]. However, it should be noted that the composition varies depending on the insects as well as the host tree from which the raw material is obtained [10].

Shellac has been used for centuries in a broader art sector, mainly to varnish, protect the surface of wooden artworks, in the field of wooden furniture restoration and musical instruments, due to its interesting features including good film-forming, ease of application, high adhesion to the wood surface, aesthetical excellence of coatings, and protective properties along with its non-poisonous nature [8, 11–13].

In more recent years, shellac has found application in very different fields (e.g. pharmaceutical industry, food treatments, children's toys, electrical insulation) because of some peculiar characteristics such as thermoplasticity, insulating properties, and, as mentioned above, low toxicity [8, 14–18].

Shellac is still known as one of the most elegant finish for furniture and currently used for restoration and refinishing wooden antiques. In particular, it is one of the most used varnishes for string musical instruments [19]. However, its use has declined due to some limitations such as the softness of the coating, photo-degradation, sensitiveness to alcoholic solvents and to pH variations [13, 20, 21].

Nanotechnology and nanomaterials are attracting increasing interest from scientists operating in different areas, including coating technologies. New concepts are now available to develop advanced materials, which can improve performance of traditional coatings and overcome their possible failures [22–24]. For instance, different inorganic nanoparticles, NPs, (e.g. ZnO, TiO_2) have been investigated as ultraviolet absorbers in order to improve photo-protection of wood coatings [2, 25–29]. In addition, the use of nanocomposites obtained from a variety of synthetic polymers and inorganic NPs have been proposed for improving physical properties of wood coatings (e.g. thermal, mechanical, resistance to decay) [2, 29–33].

In the present study, some inorganic NPs have been investigated as additives for shellac in order to improve the properties of the resulting coatings without altering to a great extent the original features of the resin, in particular chromatic properties, film-forming and water repellent behaviour, and adhesion to wood surface. Silica (SiO_2), montmorillonite (MMT), and zirconium oxide (ZrO_2) NPs were selected with the aim of mainly improving the hardness of coatings, while ZnO NPs were expected to improve the resistance to photo-degradation of the shellac matrix.

Properties of the shellac/NPs materials were studied, in comparison with plain shellac, on films obtained by casting and after application on maple wood specimens. Maple was chosen as it is diffusely used to create wooden artefacts and, in particular, as a construction material for making musical instruments [34].

A variety of experimental techniques and testing procedures were used in order to characterize all the materials and to evaluate the properties of the corresponding coatings on wood specimens. They include chromatic variation and moisture adsorption tests, contact angle measurements, thermal analysis measurements (thermogravimetric and calorimetric analyses), X-ray diffractometry (XRD), scanning electron microscopy (SEM), energy-dispersive X-ray spectroscopy (EDS), hardness and adhesion tests.

2 Experimental

2.1 General information

Dewaxed natural shellac (food quality) was purchased from Kremer-Pigmente and used without any further purification.

Ethanol (99% EtOH) supplied by Sigma-Aldrich was used as a solvent for preparing shellac stock solutions (100 and 200 g/L). Silica NPs (SiO_2, ~5 nm), zinc oxide NPs (ZnO, ~100 nm), and zirconium oxide NPs (ZrO_2, <100 nm) were supplied by Sigma-Aldrich and used without any further purification. Dellite® HPS is a natural occurring Na-montmorillonite (MMT) which was supplied by Laviosa Chimica Mineraria S.p.A. (Livorno, Italy).

Maple wood specimens (5 × 5 × 0.5 cm) were kindly provided by Civica Scuola di Liuteria (Milan, Italy).

Optical microscope observations of wood specimens and of coating films deposited on glass supports were carried out using a light-polarized microscope Olympus BX51TF, equipped with Olympus TH4-200 lamp (visible light) and Olympus U-RFL-T (UV light).

X-ray powder diffraction (XRD) measurements were taken using a Bruker D5005 diffractometer with the CuKα radiation, graphite monochromator, and scintillation detector.

Scanning electron microscopy (SEM) images (backscattered electron, BSE) and energy-dispersive X-ray spectra (EDS) were collected by using a Tescan FE-SEM, MIRA3 XMU series, equipped with a Schottky field emission source, operating in both low and high vacuum. Samples were gold-sputtered using a Cressington sputter coater 208HR.

Thermogravimetric measurements (TGA) were taken by a Q5000 apparatus (TA Instruments) under air flux (10 ml/min) in a platinum pan by heating about 10 mg of sample from room temperature to 700 °C (heating rate 5 K/min). Differential scanning calorimetry (DSC) was performed by a Q2000 apparatus (TA Instruments) by heating about 10 mg of powder in an open aluminium crucible from −50 to 250 °C (heating rate 5 K/min) under air flux (50 ml/min). Three independent measurements were taken on each sample. The temperature accuracy of the instrument is ±0.1 °C, the precision is ±0.01 °C, and the calorimetric reproducibility is ±0.05%.

2.2 Nanoparticles dispersions

The envisaged NPs were dispersed in EtOH shellac solution (200 g/L) by using a Badeline Sonoplus HD 2070 Ultrasonic Homogenizer. The dispersion time was 5 min with power set at 50%. The resulting mixtures obtained by dispersing silica, zirconium oxide Na-montmorillonite, and zinc oxide NPs were labelled as, SH + Si, SH + Zr, SH + MMT, and SH + Zn, respectively. Dispersions containing 2% of SiO_2, MMT, and ZnO, and 1% of ZrO_2 were used for the investigation described in this paper. Addition of larger amounts of NPs to shellac solutions resulted in non-homogeneous dispersions, which were not investigated.

All dispersions were used immediately after their preparation in order to avoid any possible NPs precipitation and to provide a good reproducibility for the further tests.

The kinetic stability of dispersions was determined by measuring their absorbance (A) at 600 nm. Measurements started immediately after the preparation of the dispersions, and A was monitored as a function of time for up to 60 min. Cary Varian 50 scan ultraviolet/visible spectrophotometer and 10-mm path-length quartz cuvettes were used. The relative kinetic stability parameter (KS%) of considered dispersions was calculated using the following formula [35, 36]:

$$KS\% = \{1 - [(A_0 - A_t)/A_0]\} \times 100$$

where A_0 = starting absorbance at 600 nm and A_t = absorbance at a given time at 600 nm.

2.3 Preparation of coating films and treatment of wood specimens

Films of native and modified shellac were prepared by pouring shellac solution or shellac/NPs dispersions (5.0 ml) into levelled PTFE frames (area of casting 5 × 7.5 cm, depth 1 mm) and allowing solvent to evaporate at room temperature (20 °C) for 24 h. After that, the resulting films were carefully removed from the film holder and their thickness was measured by a Borletti (Milan, Italy) micrometre. Samples for XRD experiments were obtained by preparing films on glass supports by casting.

Treatment of wood specimens was performed according to recommendations provided by Civica Scuola di Liuteria. Before treatment, maple wood specimens were smoothed by abrasive paper sheets (progressively from 400 to 1000 mesh) similarly to the real cases [37] and cleaned to remove dust. After smoothing, pores filling was performed in order to have a regular surface before applying varnish. In this work, satisfactory pores filling was obtained by using a less concentrated shellac solution (100 g/L in ethanol), which was applied two times by brushing (brush direction of second application was perpendicular to the first one). After complete drying of wood surface, specimens were treated with the different varnishes (shellac solution and shellac/NPs dispersions): In any case, the treatment was performed by consecutively applying the varnish for 15 times with a special brush (Martora Kolinsky). The direction of brush in each application was perpendicular to the pervious one in order to obtain as much as possible a regular coating surface. Specimens treated on one 5 × 5 cm side were used for most of the experiments, while fully coated (treated on all sides) specimens were used for moisture absorption tests.

2.4 Testing methods

All tests on treated wood were performed by examining three different specimens for each treatment.

Colour measurements were taken by using a Konica Minolta CM-2600d spectrophotometer, determining the L^*, a^*, and b^* coordinates of the CIELAB space, and the global chromatic variations ΔE^*, according to the UNI EN 15886 protocol [38]. Contact angle measurements on the wood specimens were taken by a CAM 200 apparatus (KSV Instruments).

Gloss measurements were taken using a Macbeth statistical NOVOGLOSS instrument (reflection angles of 20° and 60°), according to the corresponding ASTM D523 standard test [39].

Five measurements were taken on each specimen area for colorimetric, gloss, and contact angle determinations, and all the given results are average values.

The moisture adsorption test was carried out by placing fully coated wood specimens in a controlled humidity environment at a constant temperature until equilibrium [40]. After drying samples until constant weight, they were placed in desiccators containing different salts that provided various relative humidity levels (RH). In particular, RH% levels corresponding to 32, 75, and 93% were obtained by magnesium chloride, sodium chloride, and potassium nitrate, respectively. The samples were equilibrated at each condition for 10 days at 25 ± 2 °C, and then, they were immediately weighted. The weight gain of the samples was recorded and ascribed to the adsorbed humidity.

Pencil hardness test was performed on treated wood specimens as well as on coating films according to ISO 15184:1998 standard [41]. Coating adhesion on wood surface was evaluated by tape test according to the ASTM D3359 standard [42]. In particular, perpendicular cuts were performed on the dry surface of treated wood specimens by using a cutting tool made by URAI (Milan, Italy). Thereafter, several pieces (12.5 cm^2) of adhesive tape (transparent tape, SYROM, Italy) were stuck on the cut surface, smoothed with gentle finger pressure, and rapidly removed by pulling at an angle of 90°. All the results were analysed according to the standard method.

Artificial ageing were carried out on coated wood specimens and on coating films by a 2 × 20 W UV lamp apparatus (Helios Italquartz, Milan, Italy). Samples were situated at a distance of 15 cm from the lamps (radiant flux = 16.7 W/m^2; T = 25 °C; RH = 30%) and irradiated for a total time of 520 h.

3 Results and discussions

3.1 Preparation of shellac/nanoparticles dispersions

Despite both waxed and dewaxed shellac are commonly used for real applications in wood protection treatments, dewaxed shellac was selected for the present study. In fact, a preliminary investigation on the resin properties highlighted some drawbacks of the waxed shellac, mainly connected to its limited solubility, which discouraged its use in laboratory-scale experiments.

Two different species of dewaxed shellac (food and non-food quality) were also preliminarily considered, although "food label" resin was finally chosen due to the better quality of the corresponding coating films, evaluated by optical microscope.

The envisaged inorganic NPs were dispersed into ethanol shellac solution (200 g/L) by using an ultrasonic homogenizer.

Kinetic stabilities of NPs dispersed in shellac solution were evaluated by UV/visible spectroscopy, by monitoring absorbance of dispersions at 600 nm as suggested by the literature method [35, 36]. Aggregation of nanoparticles, which represents the main process causing instability, may induce precipitation with a consequent decreasing of absorbance. Figure 1 shows the relative kinetic stability changes along a time range of 60 min after preparation of selected shellac dispersions. This time range was considered long enough to allow a standard application of the dispersions. The KS% parameter values after 1 h were close to 100% for ZnO and ZrO_2 dispersions, indicating a very good stability. In the case of SH–Si, value of relative kinetic stability slightly decreased (to about 90%) after 1 h. Shellac/MMT dispersion showed a different behaviour, as KS% dropped down to less than 50% after 60 min, revealing that MMT has much lower stability into shellac solution than the other NPs, as it is also suggested by precipitation that can be observed even by naked eye. However, dispersion homogeneity can be recovered by repeating the treatment by ultrasonic homogenizer.

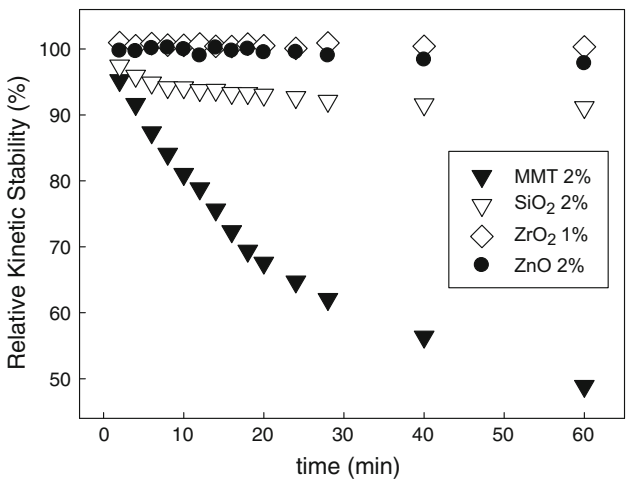

Fig. 1 Variations of relative kinetic stability (KS%) of NPs dispersions in shellac EtOH solution

The lower kinetic stability of MMT/shellac may be also due to the different morphology of starting Dellite® HPS particles and their larger dimensions if compared with the other considered NPs. Despite the considerably lower stability of MMT dispersion, it was investigated for comparing its features with the other shellac-based nanocomposites.

3.2 Coating films

Good-quality coating films were obtained by a casting procedure, as described in Sect. 2.3. Thickness measurements, taken by a micrometre in several areas of the 5 × 7.5 cm films, provided an almost constant value (0.7 ± 0.1 mm) for films obtained both from shellac solution and from shellac/NPs dispersions, indicating that the good film-forming properties of shellac are not affected by NPs.

Coating films were examined by optical microscopy mainly to assess their homogeneity. Microscope observations suggested that all NPs were spread quite homogeneously in the shellac matrix, except for MMT that formed several visible aggregates, in agreement with the lower kinetic stability of the corresponding dispersion.

3.2.1 Thermal properties

Both shellac and coating films obtained from the different shellac/NPs dispersions were investigated by TGA and DSC.

TGA analyses show that all the considered shellac-based materials are stable up to about 90 °C, *i.e.* at temperatures higher than the working temperature of the varnishes. The first mass loss (in total 15 wt%) starts at about 90 °C and can be ascribed to a release of residual solvent in shellac. This process has a very slow kinetics and goes up to 280 °C, when a second faster mass loss process starts, due to a first release of organic components from shellac. The last process starts at a temperature higher than 500 °C and ends at about 650 °C, when all the shellac is decomposed

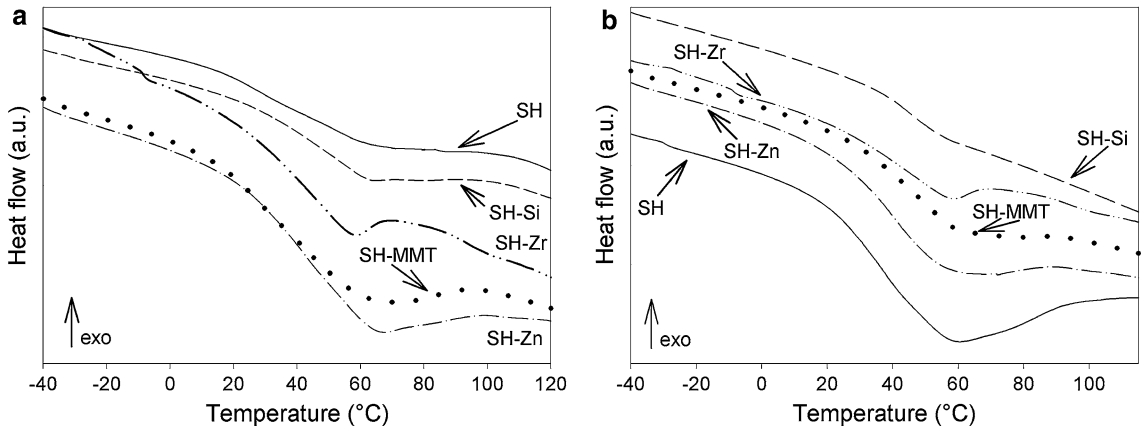

Fig. 2 DSC profiles obtained for coating films before (**a**) and after (**b**) UV ageing

and burnt out. No meaningful differences can be observed between TGA profiles of plain shellac and of its nanocomposites (curves not shown), as expected from the low NPs loading.

DSC measurements (Fig. 2) show that all the samples undergo a wide glass transition starting around room temperature and ending at temperatures higher than 75 °C, but lower than the decomposition temperature as recorded in the thermogravimetric measurements. For pure SH (Fig. 2a), the T_g value (as obtained by the TA software Universal Analysis for each measurement and averaged over the three performed runs) is 35.5 ± 0.8 °C, in good accordance with the literature data [14, 43]. For all the other samples, the T_g values are higher than 40 °C, and in particular 41.2 ± 0.8 °C for SH–MMT, 42.00 ± 0.5 °C for SH–Zn, 43.3 ± 0.5 °C for SH–Si, and 47.7 ± 0.3 °C for SH–Zr. It is worth noting that the huger T_g increase ($\Delta T_g = 12$ °C) is obtained with the SH + Zr system, despite the lower "concentration" of ZrO_2 nanoparticles (1%) dispersed into shellac. Moreover, as shown in Fig. 2, the presence of NPs changes the shape of the calorimetric profile, making the glass transition more evident and more pronounced. It should be noted that the samples are stable under natural air ageing, since the results of DSC measurements taken after 1 year of air exposure result almost overlapped with the calorimetric curves described above.

3.2.2 X-ray diffraction studies

Coating films deposited on a glass support were also investigated by X-ray diffractometry. Figure 3 shows the diffraction patterns of all the analysed materials. The broad band at about 20°, typical of the amorphous phases, is present in all the patterns and can be ascribed to shellac and to glass support. The peaks typical of crystalline phases can be observed in the diffraction patterns of SH + Zn and

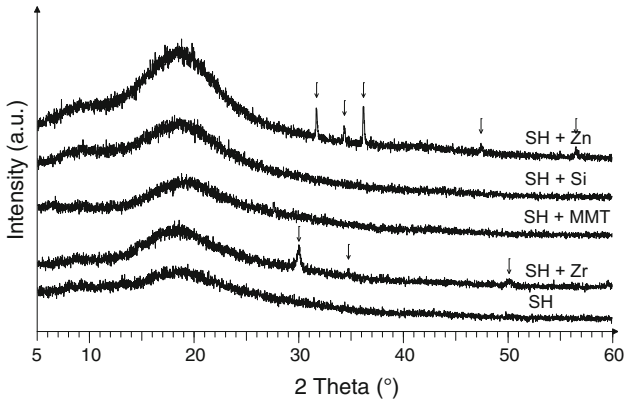

Fig. 3 X-ray diffraction patterns of investigated coating films

SH + Zr (indicated by arrows in Fig. 3) and can be ascribed to ZnO (Zincite structure) and ZrO_2 phases, in agreement with JCPDS database (SK. No: 36-1451 and SK. No: 50-1089, respectively).

On the contrary, no diffraction peaks due to crystalline phases are shown in the diffraction patterns of SH + MMT and SH + Si. In the case of montmorillonite, it could be due to the occurrence of intercalation and/or exfoliation of clay sheets by shellac oligomeric (or polymeric) chains, with the consequent decreasing of nanoparticles crystallinity. The amorphous character of silica NPs is responsible for the lack of diffraction peaks in the case of SH + Si.

3.3 Treated wood specimens

The different materials deposited on wood surface were at first examined by optical microscope in order to evaluate quality and thickness of coatings. The application performed by brushing (see Sect. 2.3) produced in any case good-quality and homogeneous layers of varnish as shown by the observations on the surface and on the cross section

of the treated maple specimens. As an example, Fig. 4a reports reflected light (UV) microphotograph taken on the cross section of a wood specimen treated with SH + Si. The coating thickness in all the examined samples is about 30 μm and comparable to that observed on a standard wood sample (Fig. 4b) treated with shellac by experts at Civica Scuola di Liuteria according to the same application procedure used in the current study.

3.3.1 Colour and gloss measurements

Wood is a special material having a natural and pleasant appearance. Therefore, most surface treatments concerning wooden artefacts (e.g. furniture, musical instruments) involve materials that allow keeping as much as possible unaltered the original aesthetic properties. Shellac, as mentioned above, has been used for centuries to varnish wooden items due to its excellent features, which include the ability to enhance the aesthetic appearance of wood surface. The presence of dispersed NPs into the examined coatings could affect this peculiar property of shellac. Hence, treated wood specimens were examined to evaluate chromatic and gloss variations induced by the different nanocomposite coatings.

Colour changes experienced by wood surface after coating application and expressed as ΔE^* values are shown in Table 1. Chromatic variations induced by shellac/NPs materials are very similar to that observed for plain shellac ($\Delta E^* = 8$), being the small variations of chromatic coordinated due to the presence of the different inorganic NPs generally within the experimental error.

Specular gloss variations determined at two different angles and expressed as Δgloss are graphically summarized in Fig. 5. As expected, all the shellac-based varnishes strongly increase the gloss of wood surface, the highest values being observed at 60° reflecting angle. Shellac/NPs coatings induce gloss enhancements that are comparable to those observed for plain shellac, with the exception of SH + Si, which is less reflective (by 25–30%) than the other investigated coatings.

3.3.2 Hydrophobic behaviour

Wood coatings, including the shellac-based ones, are expected to protect the substrate also from water and environmental humidity. The hydrophobic behaviour of the investigated shellac/NPs materials was evaluated by performing static contact angle measurements on the surface of treated maple and moisture adsorption tests on the fully coated specimens.

Contact angle (α) measured on plain shellac (see Table 1) indicates the moderately hydrophobic character of the native resin ($\alpha \approx 90°$). An increasing of α (about 20%) was observed in the case of SH + Si, while the dispersion

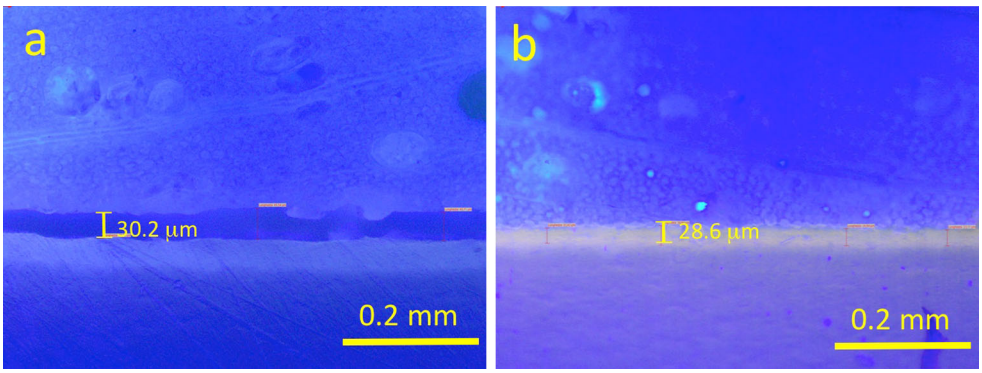

Fig. 4 Optical microscope images (reflected UV light) taken on cross sections of a standard wood board treated with shellac by expert people (**a**) and a maple specimen treated in laboratory with SH + Si according to the same procedure (**b**)

Table 1 Overall chromatic variation (ΔE^*) and contact angle values (α) measured on treated wood specimens before and after artificial ageing

Products	ΔE^*[a]		α (°)	
	Before ageing	After ageing	Before ageing	After ageing
SH	8 (±2)	13 (±1)	89 (±5)	78 (±7)
SH + Zr	10 (±1)	12 (±1)	90 (±3)	82 (±6)
SH + MMT	8 (±1)	11 (±2)	80 (±13)	75 (±6)
SH + Si	9 (±1)	12 (±1)	107 (±2)	100 (±6)
SH + Zn	9 (±2)	8 (±1)	74 (±6)	79 (±2)

[a] Variation compared to untreated wood

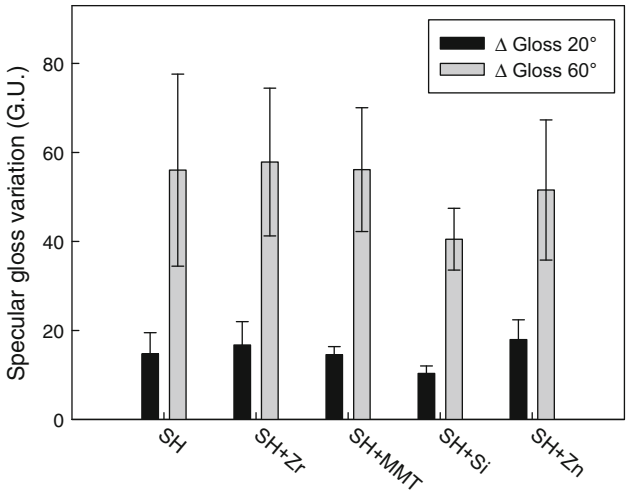

Fig. 5 Gloss variations determined on the surface of treated wood specimens

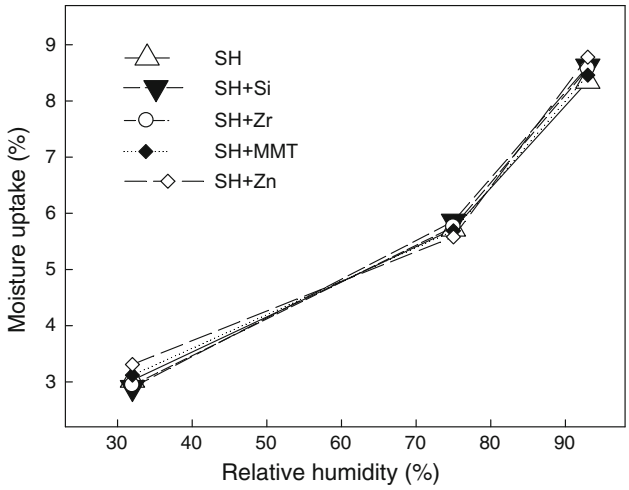

Fig. 6 Weigh increase values determined after moisture uptake tests performed on fully coated wood specimens

of ZnO NPs induced a moderate decreasing (about 15%) of the contact angle value. Differences between α values observed for the other nanocomposites (SH + Zr and SH + MMT) and plain shellac are within the experimental error.

It should be pointed out that contact angle measurements are related to an "instantaneous" and "local" water-repellence behaviour (contact angle is usually measured after a very short contact time with liquid water) and should be used with caution to assess the actual hydrophobic properties of a coating or, in general, of a protecting material [44–46]. Therefore, long-term resistance of the shellac-based coatings to water vapour was also investigated by performing moisture absorption tests on fully coated wood specimens.

Although plain shellac displays low water vapour permeability [40, 47], this property could be affected to different extents by inorganic materials dispersed in the resin matrix. To study the effect of dispersed NPs, fully coated maple specimens were exposed to controlled humidity environments and the moisture uptake values (calculated as weight increase %) determined after 10-day exposure. The test was performed at three different relative humidity levels (RH% = 32, 75 and 93%), and as expected, the moisture uptake of shellac-coated specimens increased with increasing RH% (from 3 to about 8%, see Fig. 6).

Moisture uptake values determined for all specimens coated with shellac/NPs mixtures are very similar to those observed for native shellac at any of the considered RH% levels. It suggests that the coating hygroscopicity, i.e. its behaviour towards water in the vapour phase, is not affected by the presence of dispersed inorganic NPs. It should be noted that the permeability of the shellac matrix to water vapour does not change even in the presence of MMT nanoclay, which has been largely applied to enhance the barrier properties of polymeric materials towards gases (e.g. O_2, CO_2) and water vapour [48, 49]. It could be explained on the basis of the poorly homogeneous dispersion of clay NPs into the shellac.

3.3.3 SEM–EDS studies

Surfaces of coated wood specimens were observed by electron microscopy in order to have a better insight on the microscopic properties of the coating layer, e.g. homogeneity of NPs dispersions into the solid shellac matrix.

SEM micrographs taken on wood specimens treated with the investigated shellac/NPs dispersions are shown in Fig. 7. The presence of spread white spots of different dimensions on the examined surface areas can be ascribed to the inorganic nanoparticles or to their aggregates, although the contribution of dust grains occasionally deposited on the surface during the varnish drying cannot be ruled out. The surface of coating containing MMT nanoparticles displays a less homogeneous distribution of the white spots, which have also larger dimensions. The formation of NPs aggregates in shellac/MMT dispersion is in accordance with the optical microscope observations and with the results of kinetic stability tests.

EDS analyses performed on different areas of the examined surfaces confirmed the expected elemental compositions due to the dispersed inorganic NPs. In particular, the main peaks corresponding to Si, Al and Si, and Zn are observed in the spectra obtained from the specimens treated with SH + Si, SH + MMT, and SH + Zn, respectively, beside the peaks of C and O due to the shellac organic matrix (see Fig. 7). EDS spectrum corresponding to the analysis of SH + Zr sample shows a

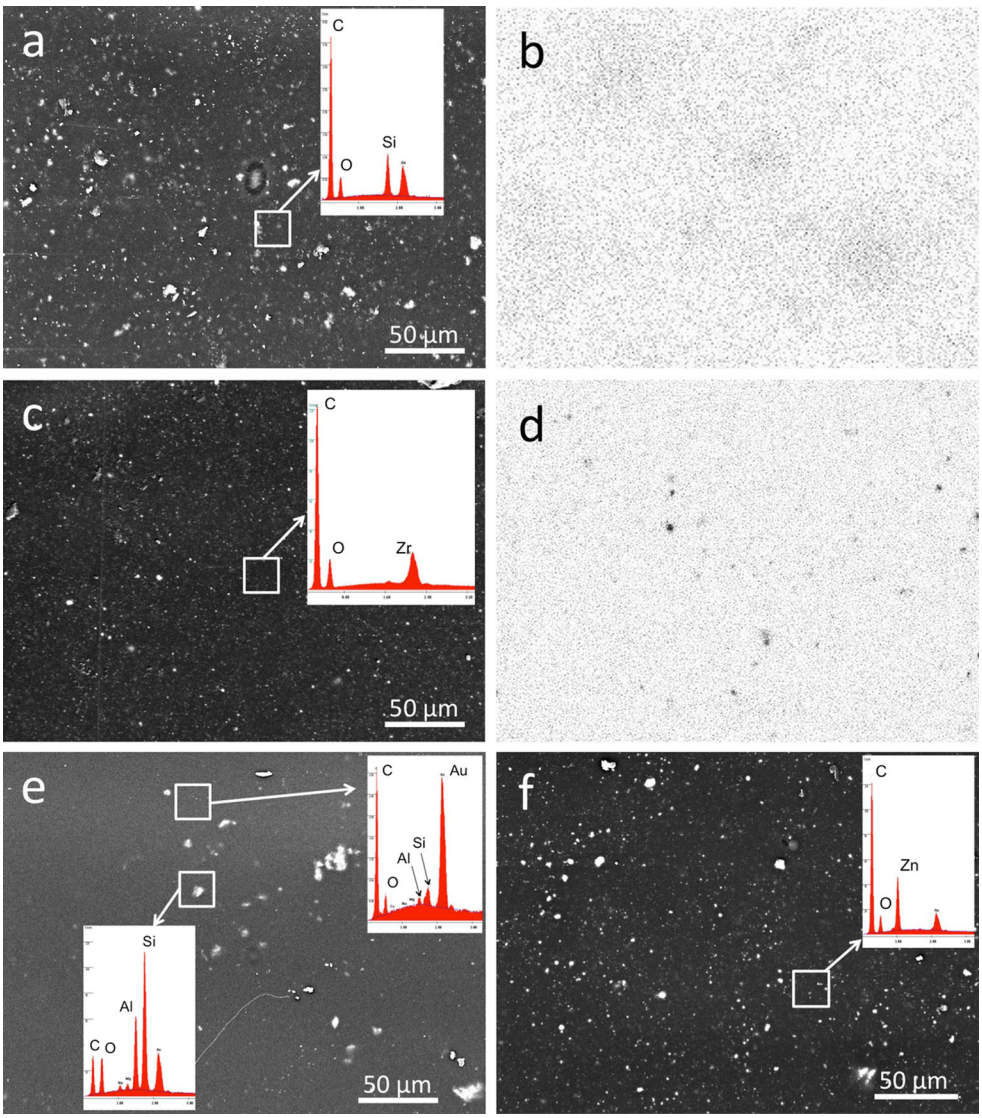

Fig. 7 Selected results of SEM–EDS experiments: SEM microphotograph taken on the surface of wood samples treated with SH + Si (**a**) and the corresponding EDS elemental mappings of silicon (**b**), SEM microphotograph taken on the surface of wood samples treated with SH + Zr (**c**) and the corresponding EDS elemental mappings of zirconium (**d**), SEM microphotographs taken on the surface of wood samples treated with SH + MMT (**e**) and SH + Zn (**f**). Selected EDS spectra are shown in the *insets* of SEM images. High concentrations of Si or Zr (and of the corresponding nanoparticles) are represented by *black spots* in the maps

broad peak centred at about 2.1 keV. It results from the overlapping of Zr-Lα and Au-M peaks expected at 2.042 and 2.120 keV, respectively [50]. The Au-M peak can be observed in the EDS spectra of all the examined samples, which have been gold-sputtered prior to carrying out the SEM–EDS experiments. However, correct identification of zirconium can be performed by using peak-fitting technique [51].

Elemental compositions are quite constant over the observed areas, supporting a general homogeneity of NPs dispersion, with the exceptions of SH + MMT material. In this case, the results of EDS analyses strongly depend on the examined area: Although Al and Si (taken as distinctive elements of MMT clay) are present all over the coating surface, the intensities of the corresponding peaks strongly increase when areas including large white spots are analysed (see Fig. 7e). It confirms again the poor homogeneity of MMT-containing coating, which is most likely caused by the aggregation of clay nanoparticles.

Distribution of NPs in the shellac matrix was also investigated by EDS elemental mapping experiments performed on treated wood. Silicon and zirconium distribution maps obtained by analysing the surfaces of specimens treated with SH + Si and SH + Zr are reported in Fig. 7b, d, respectively. Both elements and the corresponding nanoparticles (represented as black spots) are quite

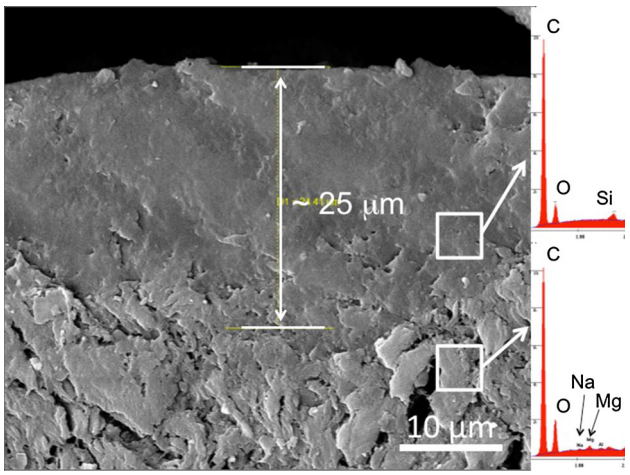

Fig. 8 SEM micrographs taken on cross section of a wood sample treated with SH + Si. EDS spectra taken on selected areas at different depth are reported in the *insets*

regularly dispersed into the organic resin, in accordance with the other, above discussed, experimental evidence.

SEM–EDS experiments were also performed on the cross section of treated wood samples. These measurements showed that coating films obtained by all the investigated varnishes are quite regular and homogeneous, as anticipated by optical microscope observations. As an example, the microphotograph taken on the cross section of a wood sample coated with SH + Si is shown in Fig. 8. Microanalyses performed at different depth from the surface showed that Si, taken as label element, is contained only in the outer layer (thickness about 25 µm) made by varnish, while it is absent in the underlying wood substrates.

Thickness values in the range 25–30 µm were detected for all the examined samples in accordance with the optical microscopy outcomes.

3.4 Performances of coatings

Shellac–NPs coatings applied on the wood surface were examined by specific tests in order to evaluate their performances in comparison with the plain shellac. In particular, surface mechanical properties (*i.e.* hardness and adhesion) and resistance to degradation induced by UV irradiation were investigated for all the treated specimens.

3.4.1 Mechanical properties

Coating hardness is an essential parameter when selecting a proper varnish for wood, in particular when protection from mechanical decay (e.g. accidental scratches) is required. Hardness of shellac and shellac–NPs coatings was evaluated by performing pencil test on all the treated wood specimens as well as on the corresponding coating films prepared as described in Sect. 2.3. Measurements were repeated three times for each sample and provided reproducible results, which are summarized in Table 2. For each material, pencil test gave the same result both when performed on film and on treated wood surface. Hardness of plain shellac coating corresponds to the intermediate hardness level "F" in the scale ranging between 9H (harder)–9B (softer) [41]. Such behaviour is not affected by the presence of ZnO NPs, as the same level of hardness is observed in the case of SH + Zn coating. On the contrary, a hardness increase is obtained in the case of SH + Si ("H" level), SH + MMT ("2H"), and SH + Zr ("3H"). It is noteworthy that ZrO_2-containing coating is considerably harder than plain shellac, although only 1% NPs are dispersed in the resin matrix.

Table 2 Results of pencil hardness test performed on the films and on the treated wood specimens

Products	Hardness	
	Films	Wood specimens
SH	F	F
SH + Zr	3H	3H
SH + MMT	2H	2H
SH + Si	H	H
SH + Zn	F	F

The adhesion behaviour of coatings was investigated by performing tape test on treated specimens. This test allows to evaluate the adhesion strength of a coating on the basis of the percent coating area removed from the examined surface that has been previously cross-cut according to the standard procedure. In all the treated wood specimens, the coating area removed by applying adhesive tape was less than 5% of the total treated area. Therefore, all the examined materials, including plain shellac, can be classified as "5B-4B" in the test scale ranging between 5B (high adhesion) and 0B (poor adhesion). It indicates that the dispersion of any of the considered inorganic NPs does not affect, or affect to poor extent, the adhesion properties of shellac on the wood surface.

3.4.2 Artificial ageing

Shellac, as commonly happens to organic materials, is subject to decay induced by long exposition to light (e.g. solar radiation) and particularly to its UV component [52]. Alteration processes promoted by light include photo-oxidation, de-esterification and crosslinking and induce variations in the chemical, mechanical, and chromatic properties of the biopolymer [52].

Maple specimens treated with plain shellac and with the different NPs dispersions, as well as the corresponding films, were irradiated by UV lamp up to 520 h in order to simulate the naturally occurring photo-degradation processes and to assess the effect of ageing on some properties of the coatings. After irradiation, treated specimens were examined by measuring contact angle and chromatic variations.

The hydrophobic behaviour of the coatings was poorly affected by the prolonged irradiation as the differences of contact angles measured before and after artificial ageing are generally within the experimental error (see Table 1).

The irradiation by UV lamp of shellac coating mainly affects L^* and b^* parameters, related to the brightness and to the blue/yellow chromatic change, respectively. The values of a^* (the parameter related to chromatic changes towards the red) undergo very small or almost undetectable variations. In particular, accelerated ageing induces a decrease in the surface brightness (negative ΔL^* values) and a chromatic change towards the yellow, (positive Δb^* values), which can be associated with the photo-oxidation processes. As a result, ΔE^* measured on the shellac surface after artificial ageing is higher (by 5 units, about 60%) than the corresponding value observed for non-aged shellac coating (see Table 1). Colour changes induced by UV irradiation are less relevant to SH + Si and SH + MMT, that both show a ΔE^* increase of about 3 units (about 35%), and for SH + Zr whose ΔE^* increases by 2 units (20%). Interestingly, no colour changes are detected in the case of SH + Zn suggesting that ZnO NPs preserve the chromatic properties of coating after prolonged irradiation of the treated specimens with UV light. This result is in accordance with the literature data, which supports the use of nanometric zinc oxide particles in the photo-protection of polymeric materials and particularly of coatings [2, 25, 26].

Films of the different materials prepared by casting were also exposed to UV lamp for 520 h and then analysed by TGA and DSC techniques.

TGA profiles of all shellac-based coatings after ageing are very similar to those obtained for unaged materials: Stability up to about 90 °C is observed also after irradiation, testifying that this treatment does not alter the behaviour of the films towards heating.

DSC analyses show that after UV ageing (Fig. 2b), a strong variation in the shape of the calorimetric profile, with a more pronounced glass transition with respect to the pure material, is evident in SH, suggesting an alteration in the biopolymer structure. The T_g values of all the samples increase, although to a different extent, suggesting that a variation in the thermal and mechanical characteristics of the films takes place upon the prolonged irradiation. In particular, the highest variation is recorded for SH–MMT and SH–Si that show a variation in the T_g as high as 5 °C, followed by pure SH and SH–Zr (3 °C). SH–Zn show a variation of only 1 °C, confirming that nanosized ZnO can be considered a promising additive for the protection of shellac coating from photo-degradation processes.

4 Conclusions

In the present work, different shellac-based coatings obtained by dispersing inorganic nanoparticles into the resin have been prepared and investigated.

The main aim of the study was to improve some specific performance of shellac when used as protective coating for wood (e.g. hardness, resistance to ageing) without altering to a much extent the aesthetical appearance of the native resin or other desirable properties. Dispersions of envisaged inorganic NPs (1–2% SiO_2, MMT, ZrO_2, ZnO) in alcoholic shellac solution were easily prepared, and their kinetic stability was generally satisfactory, with the exception of SH + MMT, probably due to the morphology and dimensions of the nanoclay particles. Optical microscopy observations and SEM–EDS experiments showed that coating films of SH + Si, SH + Zr, and SH + Zn, obtained by casting or after treatment of wood surface, display a good homogeneity, with NPs evenly dispersed into the shellac matrix. On the contrary, SH + MMT formed a less homogeneous coating with several considerable aggregates.

All the tested NPs do not affect or affect to poor extent the chromatic properties and the hydrophobic behaviour of shellac as testified by colour and contact angle measurements, as well as by moisture uptake tests. Some of the tested NPs, and particularly ZrO_2, induce a hardness enhancement of the shellac coating, while its adhesion properties are not altered by the presence of any of the considered NPs.

After artificial ageing, shellac undergoes chromatic variations (it becomes more yellow and less bright) and an increase (3 °C) in the T_g value, which can be ascribed to the photo-induced chemical processes. SH + Zn, unlike the other investigated nanocomposites, does not experience significant colour changes and display a very small increase (1 °C) in T_g after prolonged irradiation. Although the artificial ageing was not performed in particularly severe conditions (moderate power of UV lamps, relatively short exposition time), these findings indicate that ZnO NPs, when dispersed into shellac, are able to inhibit or to slow down UV-induced decay of the resin matrix. More experiments concerning artificial ageing of shellac-NPs composite under more severe conditions are currently underway, in order to better point out the role of ZnO as inhibitor of photo-degradation processes.

In conclusion, this work has shown that the addition of small amount (1–2%) of selected inorganic nanoparticles to the traditional shellac varnish may induce valuable enhancement of its performance. In particular, an increase in coating hardness can be obtained in the presence of only 1% ZrO_2 NPs, while the dispersion of ZnO NPs (2%) provides an increased resistance to decay induced by exposition to UV light. It is noteworthy that in both nanocomposites (SH + Zr and SH + Zn), the desirable features of native shellac (colour, film-forming ability, water repellence, and adhesion) are almost completely preserved.

Acknowledgements The authors gratefully acknowledge Dr. Davide Ravelli (Department of Chemistry, University of Pavia) for assistance in ageing tests and Prof. Claudio Canevari (Civica Scuola di Liuteria, Milan, Italy) for fruitful discussions and for providing shellac and maple specimens.

References

1. B. George, E. Suttie, A. Merlin, X. Deglise, Polym. Degrad. Stab. **88**, 268–274 (2005)
2. N. Auclair, B. Riedl, V. Blanchard, P. Blanchet, For. Prod. J. **61**, 20–27 (2011)
3. J.C. Schelleng, J. Acoust. Soc. Am. **44**, 1175–1183 (1968)
4. R. Rodriguez, E. Arteaga, D. Rangel, R. Salazar, S. Vargas, M. Estevez, J. Non-Cryst, Solids **355**, 132–140 (2009)
5. P.K. Bose, Y. Sankaranarayanan, S.C. Sengupta, *Chemistry of Lac*, vol. 1 (Indian Lac Research Institute, Ranchi, 1963)
6. S. Limmatvapirat, D. Panchapornpon, C. Limmatvapirat, J. Nunthanid, M. Luangtana-Anan, S. Puttipipatkhachorn, Eur. J. Pharm. Biopharm. **70**, 335–344 (2008)
7. L. Wang, Y. Ishida, H. Ohtani, S. Tsuge, Anal. Chem. **71**, 1316–1322 (1999)
8. J. Wang, L. Chen, Y. He, Prog. Org. Coat. **62**, 307–312 (2008)
9. S.K. Sharma, S.K. Shukla, D.N. Vaid, Def. Sci. J. **33**, 261–271 (1983)
10. Y. Farag, C.S. Leopold, Dissolut. Technol. **16**, 33–39 (2009)
11. E.J. Parry, *Shellac: its production, manufacture, chemistry analysis, commerce and uses* (Sir I. Pitman & Sons, London, 1935), p. 3
12. N. Umney, S. Rivers, *Conservation of furniture* (Butterworth–Heinemann, Oxford, 2003)
13. M. Licchelli, M. Malagodi, M. Somaini, M. Weththimuni, C. Zanchi, Surf. Eng. **29**, 121–127 (2013)
14. N. Pearnchob, A. Dashevsky, R. Bodmeier, J. Control. Release **94**, 313–321 (2004)
15. C.T. Rhodes, S.C. Porter, in *Encyclopedia of controlled drug delivery*, ed. by E. Mathiowitz (Wiley & Sons, New York, 1999), pp. 299–311
16. A. Baldwin, in *Edible coatings and films to improve food quality*, ed. by J.M. Krochta, et al. (Technomic Publishing Company, Lancaster, PA, 1994), pp. 25–64
17. D.P. The, F. Debeaufort, D. Luu, A. Voilley, J. Membr. Sci. **325**, 277–283 (2008)
18. J. Bai, R.D. Hagenmaier, E.A. Baldwin, J. Agric. Food Chem. **50**, 7660–7668 (2002)
19. B.H. Tai, J. Violin Soc. Am.: VSA papers. **23**, 1–31 (2009)
20. W.H. Gardner, W.F. Whitmore, Ind. Eng. Chem. **21**, 226–229 (1929)
21. S. Limmatvapirat, J. Nuntanid, M. Luangtana-Anan, S. Puttipipatkhachorn, Pharm. Dev. Technol. **1**, 41–46 (2005)
22. H. Goesmann, C. Feldmann, Angew. Chem. Int. Ed. **49**, 1362–1395 (2010)
23. H. Althues, J. Henle, S. Kaskel, Chem. Soc. Rev. **36**, 1454–1465 (2007)
24. P.M. Ajayan, L.S. Schadler, P. Braun, *Nanocomposite science and technology* (Wiley-VCH, Weinheim, 2003)
25. J. Salla, K.K. Pandey, K. Srinivas, Polym. Degrad. Stab. **97**, 592–596 (2012)
26. F. Weichelt, R. Emmler, R. Flyunt, E. Beyer, M.R. Buchmeiser, M. Beyer, Macromol. Mater. Eng. **295**, 130–136 (2010)
27. F. Aloui, A. Ahajji, Y. Irmouli, B. George, B. Charrier, A. Merlin, App. Surf. Sci. **253**, 3737–3745 (2007)
28. N.S. Allen, M. Edge, A. Ortega, G. Sandoval, C.M. Liauw, J. Verran, J. Stratton, R.B. McIntyre, Polym. Degrad. Stab. **85**, 927–946 (2004)
29. R.R. Devi, T.K. Maji, Ind. Eng. Chem. Res. **51**, 3870–3880 (2012)
30. S.K. Dhoke, R. Bhandari, A.S. Khanna, Prog. Org. Coat. **4**, 39–46 (2009)
31. M. Vlad-Cristea, B. Riedl, P. Blanchet, E. Jimenez-Pique, Eur. Polym. J. **48**, 441–453 (2012)
32. C. Sow, B. Riedl, P. Blanchet, J. Coat. Technol. Res. **8**, 211–221 (2011)
33. E. Amerio, P. Fabbri, G. Malucelli, M. Messori, M. Sangermano, R. Taurino, Prog. Org. Coat. **62**, 129–133 (2008)
34. J. Nagyvary, J.A. DiVerdi, N.L. Owen, H.D. Tolley, Nature **444**, 565 (2006)
35. M. Licchelli, M. Malagodi, M. Weththimuni, C. Zanchi, Appl. Phys. A **114**, 673–683 (2014)
36. R. Giorgi, L. Dei, P. Baglioni, Stud. Conserv. **45**, 154–161 (2000)
37. A. Turco, *Coloritura verniciatura e laccatura del legno*, 3rd edn. (Hoepli, Milan, 2005)
38. UNI EN 15886:2010, *Conservation of cultural property—test methods—colour measurement of surfaces* (Ente Nazionale Italiano di Unificazione, Milan, 2010)
39. ASTM D523-14, *Standard test method for specular gloss* (ASTM International, West Conshohocken, 2014)
40. S. Limmatvapirat, D. Panchapornpon, C. Limmatvapirat, J. Nunthanid, M. Luangtana-Anan, S. Puttipipatkhachorn, Eur. J. Pharm. Biopharm. **67**, 690–698 (2007)
41. ISO 15184:1998, *Paints and varnishes—Determination of film hardness by pencil test* (International Organization for Standardization, Genève, 1998)
42. ASTM D3359-09e2, *Standard test methods for measuring adhesion by tape test* (ASTM International, West Conshohocken, 2009)
43. N. Poovarodom, W. Permyanwattana, J. Thermoplast. Compos. Mater. **28**, 597–609 (2015)
44. A. Tsakalof, P. Manoudis, I. Karapanagiotis, I. Chryssoulakis, C. Panayiotou, J. Cult. Herit. **8**, 69–72 (2007)
45. M. Brugnara, C. Della Volpe, A. Penati, S. Siboni, T. Poli, L. Toniolo, Ann. Chim. **93**, 881–888 (2003)
46. M. Brugnara, E. Degasperi, C. Della Volpe, D. Maniglio, A. Penati, S. Siboni, L. Toniolo, T. Poli, S. Invernizzi, V. Castelvetro, Coll. Surf. A **241**, 299–312 (2004)
47. G.S. Banker, G.A. Agyilirah, in *Polymers for controlled drug delivery*, ed. by P.J. Tarcha (CRC Press, London, 1999), pp. 39–66
48. S. Sinha Ray, M. Okamoto, Prog. Polym. Sci. **28**, 1539–1641 (2003)
49. S. Pavlidou, C.D. Papaspyrides, Prog. Polym. Sci. **33**, 1119–1198 (2008)

50. A.C. Thompson, D. Vaughan, *X-ray data booklet*, 2nd edn. (Lawrence Berkeley National Laboratory, University of California, Berkeley, 2001)
51. H. Younan, L. Binghai, M. Zhiqiang, J. Teong, in Proceedings of 15th International Symposium on the Physical and Failure Analysis of Integrated Circuits, (IEEE Xplore Digital Library, 2008), http://ieeexplore.ieee.org/stamp/stamp.jsp?tp=&arnumber=4588206. Accessed 10 June 2016
52. C. Coelho, R. Nanabala, M. Ménager, S. Commereuc, V. Verney, Polym. Degrad. Stab. **97**, 936–940 (2012)